



HHS Public Access

Author manuscript

Nat Cell Biol. Author manuscript; available in PMC 2009 November 01.

Published in final edited form as:

Nat Cell Biol. 2009 May ; 11(5): 637–643. doi:10.1038/ncb1870.

BMP heterodimers assemble hetero-type I receptor complexes that pattern the DV axis

Shawn C. Little and Mary C. Mullins

Department of Cell and Developmental Biology, University of Pennsylvania School of Medicine, 1211 BRBII/III, 421 Curie Blvd., Philadelphia, PA 19104-6058, USA

Abstract

Patterning the embryonic dorsoventral (DV) axis of both vertebrates and invertebrates requires signaling via Bone Morphogenetic Proteins (BMPs)¹. Although a well studied process, the physiologically relevant BMP signaling complex in the *Drosophila* embryo is controversial^{2, 3} and generally inferred from cell culture studies, and has not been investigated in vertebrates. Here, we demonstrate that DV patterning in zebrafish requires two classes of nonredundant type I BMP receptors, Alk3/6 and Alk8. We show under physiologic conditions *in the embryo* that these two type I receptor classes form a complex in a manner that depends on both Bmp2 and Bmp7. We found that both Bmp2/7 heterodimers, as well as Bmp2 and Bmp7 homodimers, form in the embryo. However, only recombinant ligand heterodimers can activate BMP signaling in the early embryo, whereas a combination of Bmp2 and Bmp7 homodimers cannot. We propose that only heterodimers, signaling via two distinct classes of type I receptor, possess sufficient receptor affinity in an environment of extracellular antagonists to elicit the signaling response required for DV patterning.

BMP ligands signal as dimers by assembling a quadripartite transmembrane serine/threonine kinase receptor complex consisting of two type I and two type II receptors. Complex assembly initiates a phosphorylation cascade activating the BMP responsive Smads^{1/5/8/4}. In the *Drosophila* embryo, DV patterning requires two BMP ligands, Screw and Decapentaplegic, and two type I receptors, Saxophone and Thickveins⁵. Vertebrate embryos also express multiple ligands and type I receptors^{1, 6}: Bmp2b and Bmp7 play genetically equivalent, nonredundant roles in zebrafish⁷, and three type I receptors, *alk3a*, *alk6a*, and *alk8* (also known as *bmpr1a*, *bmpr1b*, and *acvr1*) are expressed maternally and ubiquitously^{8–10}, as are two duplicate co-orthologs, *alk3b* (*bmpr1ab*)¹¹ (not shown) and *alk6b* (see Supplementary Information, Fig. S1 online). Whereas DV patterning requires *alk8*^{12, 13}, the functional orthologue of *alk2* in mammals and frogs, the highly similar *alk3/6* class of receptors has not been investigated by loss-of-function in zebrafish DV patterning. To assess the contribution of these genes, we knocked down gene function in wild-type (WT) embryos with translation-blocking morpholinos (MOs) (Supplementary Information, Fig. S2).

Users may view, print, copy, and download text and data-mine the content in such documents, for the purposes of academic research, subject always to the full Conditions of use:http://www.nature.com/authors/editorial_policies/license.html#terms

Correspondence should be addressed to M.C.M. (mullins@mail.med.upenn.edu).

Knockdown of *alk3b* alone mildly decreased BMP signaling, inducing morphological phenotypes of weak (class 1 (C1) or C2) to moderate (C3) dorsalization¹⁴, depending on the amount of MO supplied (Supplementary Information, Fig. S3). Conversely, no amount of MOs against *alk3a*, *alk6a*, or *alk6b*, either singly or in any combination, caused dorsalized phenotypes. However, dorsalization by *alk3b* MO was enhanced by co-knockdown of *alk3a*, *alk6a* or *alk6b*, with triple and quadruple knockdown causing increasingly severe (C4 and C5) dorsalization, as judged morphologically and by whole mount in situ hybridization (Fig. 1a-l and Supplementary Information, Fig. S3). Typical of BMP mutant dorsalization, Alk3/6 knockdown caused expansion of dorsal cell fates, accompanied by reduction of ventral cell fates during gastrulation and early somitogenesis (Fig. 1a-l). Combined loss of Alk3/6 caused pronounced reduction in phosphorylated (P-)Smad1/5 levels identical to that seen in *bmp7* null mutant embryos (Fig. 1m and Supplementary Information, Fig. S3). Co-injection of mRNA encoding human Alk3 or mouse Alk6 rescued P-Smad1/5 levels (Fig. 1m) and rescued the dorsalized phenotypes (Fig. 2a-g), demonstrating the specificity of these MOs. These results show that *alk3a* and *alk6a/b* function redundantly to *alk3b* in DV patterning and that the combined reduction of *alk3* and *alk6* gene function abrogates all BMP signaling during gastrulation.

We next investigated if the *alk3/6* and *alk8* type I receptors have overlapping functions in DV patterning by examining if their loss-of-function phenotypes are enhanced when they are both partially deficient. We found that Alk3b knockdown did not enhance the C2 dorsalized phenotype of *alk8* zygotic mutants^{12, 13}, and the C3 phenotype induced by strong *alk3b* knockdown was not enhanced by loss of *alk8* (Supplementary Information, Fig. S4a). Knockdown of *alk3a*, *alk6a*, or *alk6b* did not further dorsalize *alk8* mutants (not shown). Moreover, injection of WT *alk3a* mRNA at amounts that rescue *alk3/6* morphants failed to rescue *alk8* morphants (Fig. 2g) or mutants (Supplementary Information, Fig. S4b), and increasing amounts dorsalized embryos (Supplementary Information, Fig. S4b, also seen for *alk6a*¹²). Similarly, *alk8* RNA did not rescue the loss of *alk3/6* when supplied in any amount, including levels that rescue *alk8* mutants (Fig. 2g and Supplementary Information, Figure S4c). Maternal-zygotic *alk8* mutants display severe dorsalization¹³, similar to that seen when Alk3/6 is depleted. We conclude that Alk3/6 and Alk8 fulfill mutually exclusive roles, functioning non-redundantly in DV patterning. Interestingly, the independent requirement of these two receptor classes to elicit BMP signaling during gastrulation parallels the requirement for two non-redundant BMP ligands⁷.

To account for the requirement of two BMP ligands in *Drosophila* DV patterning, two models each with supporting evidence have been proposed. One model supports heterodimer-based signaling², whereas the other supports pairs of homodimers mediating signaling³. In vertebrates, no study has determined the nature of mature dimeric BMP ligands required for DV patterning. We performed immunoblots on lysates of early gastrula embryos injected with mRNA of either epitope-tagged HA-Bmp7 or HA-Bmp2b (Supplementary Information, Fig. S2) at biological levels that rescue respective mutants, but do not ventralize them. Under reducing conditions, we observed bands migrating at the expected sizes for Bmp7 and Bmp2b monomers (Fig. 3a, lower panel). Under non-reducing conditions, we found HA-Bmp7 at approximately 39, 37, and 35 kDa (lane 2). In embryos

depleted for Bmp2b by morpholino15, the 35 kDa band was largely eliminated (lane 3). HA-Bmp2b migrated as two bands at 35 and 34 kDa when produced from WT embryos (lane 4). However, in *bmp7* protein null mutant embryos, the 35 kDa signal was absent (lane 5). Under reducing conditions, no bands appeared between the 37 and 25 kDa molecular weight markers. These results suggest that the 35 kDa band corresponds to Bmp2b-Bmp7 heterodimers with the tagged BMP monomer heterodimerizing with an endogenous BMP monomer.

To directly investigate if both homodimers and heterodimers form in the embryo, we co-injected RNA for FLAG and HA epitope-tagged ligands, then performed anti-HA immunoprecipitation (IP) followed by Western blot for FLAG. We found that Bmp7 homodimers migrate as two species of 39 and 37 kDa, but not 35 kD (Fig. 3b, lane 2). Differential post-translational modification or alternate cleavage sites of Bmp7 may cause Bmp7 homodimers to appear at two sizes^{16, 17}. Bmp2b homodimers are found at 34 kDa (lane 4), whereas only heterodimers appear at 35 kDa (Fig. 3b, lane 3). Therefore, Bmp7 homodimers, Bmp2b homodimers, and Bmp2b-Bmp7 heterodimers derived from microinjected mRNAs form in the zebrafish embryo.

In *Drosophila*, individual homodimers can signal in parallel in DV patterning possibly by independently assembling receptor complexes containing only one class of type I receptor³. Another study in *Drosophila* supports ligand heterodimers oligomerizing heteromeric type I complexes in DV patterning². To test the functional requirement for two homodimers versus heterodimers in the zebrafish embryo, we examined if recombinant Bmp7 and Bmp2 homodimers or Bmp2-Bmp7 protein heterodimers could activate BMP signaling in the absence of endogenous Bmp2b. We disrupted signaling with *bmp2b* MO, then injected either a combination of Bmp2 and Bmp7 homodimers or Bmp2-Bmp7 heterodimers at 3 to 4 hours post-fertilization (hpf) into the yolk cytoplasmic layer (YCL) underlying the blastoderm, then examined P-Smad1/5 distribution. Whereas Bmp2b depletion eliminated nuclear P-Smad1/5 (Fig. 4a, b), we found that heterodimer treatment activated BMP signaling and nuclear localization of P-Smad1/5 (Fig. 4d, e). In contrast, the homodimer mixture did not activate signaling in the embryo (Fig. 4c), although they did induce phosphorylation of Smad1/5/8 when applied to COS7 or 293T cells in culture (data not shown). Interestingly, the heterodimer could restore the gradient of BMP activity (Fig. 4e) normally seen in WT embryos (Fig. 4a18).

We conclude that homodimers although present do not elicit signaling, and that, consistent with the genetic requirement for two ligand genes, heterodimers exclusively activate BMP signaling in the zebrafish embryo.

To determine in vertebrates if heterodimers can induce heteromeric type I receptor association, we co-injected WT or ligand-depleted embryos with mRNA encoding functional epitope-tagged Alk3a and Alk8 at levels that rescue *alk3a/b* morphants or *alk8* mutants, and performed IP after treating embryos at early gastrulation with the reversible, membrane impermeable crosslinker DTSSP19. We could co-IP Alk3a-HA with Alk8-FLAG (Fig. 5a, lane 4) and, conversely, co-IP Alk8-HA with Alk3a-FLAG (Fig. 5b, lane 7). Neither Alk3a-FLAG nor Alk8-FLAG associated with Alk4, a Type I receptor for Nodal-

related TGF- β ligands (Fig. 5a), or with an unrelated transmembrane receptor protein, Unplugged/MuSK (not shown). Therefore, Alk3a and Alk8 were found in crosslinked complexes in WT embryos. Importantly, in embryos deficient of either Bmp2b (by morpholino (as shown) or protein null mutant (not shown)) or Bmp7 (by null mutation as shown), association of Alk8-HA and Alk3a-FLAG was disrupted (Fig. 5b, lanes 7–9). Additionally, Alk3a and Alk8 form homo-oligomeric complexes. However, in contrast to heteromeric complexes, homomeric association is not ligand dependent (Supplemental Information, Fig. S5). TGF- β type I receptors homo-oligomerize in tissue culture in the absence of ligand, reflecting intracellular complex formation that persists on the cell surface, but is incapable of signaling^{20, 21}. This self-association cannot drive BMP signaling in the zebrafish embryo, even in the presence of BMP homodimers. Therefore, two classes of type I receptor associate in the embryo only in the presence of both Bmp7 and Bmp2b, supporting a model in which the obligate BMP signaling complex contains both Alk3/6 and Alk8 Type I receptors whose assembly is mediated by Bmp2-Bmp7 heterodimers.

Prior studies have determined that homodimeric Bmp2/4 ligands bind the type I receptors Alk3/6 with high affinity and recruit the type II receptor poorly: the K_D of Bmp4 homodimers for Alk3 is between 250–900 pM^{22, 23}, whereas the K_D for Bmp2 binding to either BMPRII or ActRII type II receptors is only 50–100 nM²⁴. Conversely, Bmp7 homodimers possess high affinity for the type II receptor and, like the TGF- β ligand itself, do not bind their type I receptors, the Alk2/8 class, unless bound to the type II receptor^{25, 26}. In TGF- β homodimers, the two sites that bind each type I receptor are identical, whereas in a Bmp2-Bmp7 heterodimer the two type I interaction domains are distinct. The site formed by the Bmp7 β -strands and the Bmp2 α -helix²⁷ shows 96% similarity to the high affinity Alk3 binding site found in Bmp2 homodimers, and we therefore predict it to bind Alk3/6. The structure of Alk2/8 bound to ligand has not been determined, so we cannot assess the nature of its binding to the remaining type I site of the Bmp2-Bmp7 heterodimer (Fig. 5c), although it is interesting to speculate that Alk2/8 could have higher affinity for it than a Bmp7 homodimer. The Alk3/6 binding site is adjacent to the high affinity type II interaction domain of Bmp7 (Fig. 5c), and structural considerations suggest that this type II receptor activates the adjacent Alk3/6 receptor in the same half of the ligand²⁸. The presence of both Bmp2 and Bmp7 moieties in the same ligand thus may endow heterodimers with a higher combined affinity for both the type I and type II receptors, thus facilitating formation of active signaling complexes by heterodimers. Interestingly, this may also account for the higher activity of BMP heterodimers found in some biological assays^{29–31}.

Vertebrate embryos express multiple ligand-binding antagonists during DV patterning. These antagonists are essential to prohibit BMP ventralizing signals in dorsal regions and generate a gradient of BMP activity, which patterns ventrolateral tissues^{32, 33}. Bmp4 homodimers bind to these antagonists with comparable or stronger affinity than to their receptors: the estimated K_D of Bmp4 homodimers for Noggin is 20 pM, 200 pM for Chordin, and 600 pM for Cerberus^{34–36}. In vitro, Chordin shows similar affinity for Bmp4-Bmp7 heterodimers as for Bmp4 homodimers³⁴, and Chordin antagonizes heterodimers in *Xenopus* animal caps³⁷. However, antagonists other than Chordin could bind heterodimers with lower affinity than homodimers. BMP antagonism requires only a bimolecular interaction between one ligand and one antagonist molecule, which is thermodynamically

more likely than the assembly of the five molecule complex required for BMP signaling. A multitude of BMP-binding factors are expressed both dorsally and ventrally that limit ligand availability³⁸. Therefore, we expect that signaling will be elicited only from ligands with a robust ability to assemble functional receptor complexes. The competition for ligand binding between antagonists and receptors, combined with the reduced affinity of homodimers for one type of receptor, possibly in conjunction with reduced affinity of BMP heterodimers for some antagonists, might thereby account for the impotency of homodimers and the exclusive requirement for heterodimers in DV patterning (Fig. 5d).

METHODS

Strains

Mutant strains used were *lost-a-fin^{tm110b}* (*alk8*) (a putative null allele, genotyped as described¹³), *snh^{sb1aub}* (a protein-null allele of *bmp7*)⁷, and *swirl^{tdc24}* (a protein-null allele of *bmp2b*)³⁹. To obtain clutches of homozygous mutant *snh^{sb1aub}* and *swirl^{tdc24}* embryos, we intercrossed homozygous adults that had been rescued as embryos by *smad5* mRNA injection^{7, 40}.

Cloning of *alk6b*

Database searches revealed one EST (GenBank acc. AW116517) most closely related to zebrafish *alk6a*. TBLASTN searches using *alk6a* revealed several similar sequences present in the zebrafish genome, which were not identical to any known genes. RT-PCR was performed on one-cell stage embryo RNA using primers designed to obtain a full open reading frame. 5' RACE was performed to obtain untranslated 5' sequence using Generacer kit (Invitrogen). Several clones were sequenced and used to assemble the sequence of *alk6b* as given in Supplementary Fig. 1.

Epitope-tagged constructs

Sequences of the epitope junctions for each receptor and ligand construct are given in Supplementary Fig. 5. All constructs were tested for their ability to rescue mutants (for *bmp2b*, *bmp7*, *alk8*) or morphants (for *alk3a*). C-terminal epitope tagged receptor constructs were generated. For FLAG tagging, PCR was used to place *alk3a* and *alk8* into a derivative of pCS2+ containing two FLAG epitopes (a gift of M. Deardorff and P. Klein). For HA tags, we carried out PCR using 3' primers bearing a single HA epitope and placed the resulting products into pCS2+.

For ligands, we employed "seamless" cloning methodology⁴¹ to place epitopes C-terminal to the pro domain and N-terminal to the mature monomer. PCR was used to separately amplify the pro domains and mature ligands. The 3' portion of the pro domain PCR product contained a glycine linker followed by the 5' sequence of either the HA or FLAG epitopes, followed by the recognition site for the type IIS restriction endonuclease BsmBI, which cleaves outside of its recognition sequence. The 5' portion of the mature ligand PCR product encoded the BsmBI site, the remainder of either the FLAG or HA epitope, followed by another glycine linker sequence. The PCR products were digested with BsmBI, ligated, PCR performed across the junction, and the resulting products placed into pCS2+.

Morpholino and mRNA injection

All injections were performed on multiple occasions. Morpholinos against *alk3/6* were obtained from Gene Tools LLC. Binding sites are shown in Supplementary Fig. 2. For *alk3b* knockdown experiments, we injected simultaneously equal amounts of two morpholinos (MO1 and MO3) each at half the concentration given. For *alk6b* knockdown, we show combined results using either of two MOs individually, which behaved similarly to each other. To allow embryo survival to one day post-fertilization for the quadruple knockdown and rescue shown in Fig. 2j, we injected crosses of homozygous *p53* mutant females to heterozygous *p53* males⁴². *bmp2b* MO15 was injected at 0.8 ng per embryo. For *alk8* knockdown, we used 12 ng *alk8* MO3 (identical to *alk8morph212*) with 3 ng *alk8* MO2 (5' TGCCTTTCAGTATTCGCACAGCCAG 3') per embryo. Morpholinos were diluted in Danieau buffer and injected at 1 nL per embryo to provide the amounts indicated in each experiment. mRNA morpholino rescue experiments were performed as described⁴³.

All mRNAs were injected at rescuing levels: 50 pg *bmp7*, 15 pg *bmp2b*, 10 pg *alk3a*, 30 pg *alk8*. HA, FLAG, and non tagged versions behaved similarly when assayed for activity in the embryo. For Alk4-HA controls, we were unable to detect by Western epitope-tagged WT zebrafish Alk4-HA or human Alk4-HA. However, a kinase-ablated hAlk4(KR)-HA was detectable (a gift from M. Whitman), presumably because it is not endocytosed and/or degraded upon activation of signaling¹⁹. We injected *alk4(KR)-HA* mRNA at levels sufficient to block mesoderm induction (50 pg per embryo, not shown). All mRNAs were transcribed in vitro using SP6 mMessage mMachine (Ambion).

Crosslinking and immunoprecipitation

For all protein analysis, embryos were injected with mRNA encoding epitope-tagged factors at the one cell stage, manually dechorionated, and allowed to develop until early gastrulation (shield stage, 6 hpf). The amount of mRNA injected was the amount needed to rescue respective mutants or morphants. The mRNA amount determined the number of embryos processed for each IP, with more embryos required in cases where relatively less RNA was injected per embryo.

Figure 3 lane #	number of embryos	Figure 5 lane #	Number of embryos	Figure S5 lane #	Number of embryos
a2, 3	50	a2-4	250	a4-8	250
a1, 4, 5	100	a8-10	250	b4-8	50
b1, 2	250	b5-9	150		
b3	150				
b4	500				

For crosslinking of receptors, embryos at shield stage were placed in 0.2 mL modified Ringer's solution (116 mM NaCl, 3 mM KCl, 4 mM CaCl₂, 1 mM MgCl₂, 5 mM HEPES pH 7.8) containing 5 mM DTSSP (Pierce). Embryos were incubated at 28°C for 1.5 hours, then transferred into Ringer's plus 50 mM Tris pH 7.6 and incubated at room temperature for 20 minutes to quench the crosslinking reaction. No crosslinking was performed for

ligand IPs. Embryos were transferred into 0.2 to 0.4 mL lysis buffer (50 mM Tris pH7.5, 150 mM NaCl, 1 mM EDTA, 10% glycerol, 1% Triton X-100, and protease inhibitors (Sigma P2714)), disrupted manually in Kontes tubes with pestle, incubated on ice 30 minutes with vortexing every 5 minutes, clarified by 30 minute centrifugation at 14krpm, and supernatant transferred to fresh tubes.

IP for HA epitope was performed using 2 μ l packed resin per sample anti-HA affinity matrix (Roche 11815016001) added directly to embryo lysates. IP for FLAG epitope was performed using 2.5 μ l packed gel per sample anti-FLAG M2 affinity gel (Sigma A2220) prepared by washing four times briefly in excess TBST, once for 10 minutes in 0.1M glycine pH 3.5, four times briefly in TBST, and once in lysis buffer. Samples were exposed to affinity gel overnight at 4°C with gentle mixing. Receptor IPs were washed at 4°C six times in RIPA (50 mM Tris pH 8.0, 150 mM NaCl, 1% NP-40, 0.5% deoxycholate, 0.1% SDS, protease inhibitors) for one hour per wash, followed by one overnight wash. Ligand IPs were washed three times briefly in wash buffer (50 mM Tris pH 7.6, 150 mM NaCl, 1% Triton X-100, protease inhibitors). After washes, affinity resin was left in 10 μ l of buffer, to which was added 10 μ l 2X SDS loading buffer. Samples were stored at 4°C until SDS-PAGE analysis.

Western blot analysis

IPs of crosslinked receptors were analyzed on 8% SDS-PAGE gels after adding β -mercaptoethanol to the IPs at 5%. IPs of ligands were analyzed by 12% SDS-PAGE. Nonreducing gels were run approximately one hour longer than reducing gels to obtain higher resolution of ligand species closely similar in size. Western blot analysis was performed by transferring to PVDF and, after blocking in 5% nonfat milk, probing with 1:2000 rabbit anti-FLAG (Sigma F7425) or 1:2000 rabbit anti-HA (Invitrogen 71-5500) followed by 1:2000 donkey anti-rabbit-HRP (GE Healthcare NA934V). Anti-P-Smad1/5 and anti-actin westerns were carried out as described¹⁸, except that embryos were manually dechorionated and deyolked prior to collection, only one embryo was analyzed per lane, and primary antibody was applied for only one overnight period.

YCL injection

For YCL injection, 0.8 ng *bmp2b* MO15 was injected at the one-cell stage. Between 3 and 4 hpf, YCL was injected with 3 to 4 nL of a 0.1 M KCl solution containing 0.1% BSA, 0.5% rhodamine dextran, and either 120 nM hBmp2-hBmp7 heterodimer (R&D Systems 3229-BM) alone, 60 or 120 nM zBmp2a (R&D Systems 111-BM) or hBmp2 (355-BM) with 60 or 120 nM hBmp7 (354-BP), or no ligand. Embryos were allowed to develop 1.5 hours, then fixed in 4% paraformaldehyde and processed for whole mount anti-P-Smad1/5 immunostaining and confocal imaging¹⁸.

Supplementary Material

Refer to Web version on PubMed Central for supplementary material.

Acknowledgments

We thank M. Whitman for the Alk4(KR)HA construct; L. Jing and M. Granato for myc-tagged Unplugged/MuSK; B. Holloway and J. Tucker for technical advice; S. Lu for technical support; J. Xie and the UPenn zebrafish core facility for WT embryos; S. DiNardo, T. Gupta, F. Marlow, and L. Kapp for comments on the manuscript. This work was funded by NIH grants GM56326 to M.C.M. and training grants 5 T32 GM07229-28 and 2 T32 HD007516-05 to S.C.L.

References

1. Little SC, Mullins MC. Extracellular modulation of BMP activity in patterning the dorsoventral axis. *Birth Defects Res C Embryo Today*. 2006; 78:224–242. [PubMed: 17061292]
2. Shimmi O, Umulis D, Othmer H, O'Connor MB. Facilitated transport of a Dpp/Scw heterodimer by Sog/Tsg leads to robust patterning of the Drosophila blastoderm embryo. *Cell*. 2005; 120:873–886. [PubMed: 15797386]
3. Wang YC, Ferguson EL. Spatial bistability of Dpp-receptor interactions during Drosophila dorsal-ventral patterning. *Nature*. 2005; 434:229–234. [PubMed: 15759004]
4. Feng XH, Derynck R. Specificity and versatility in tgf-beta signaling through Smads. *Annu Rev Cell Dev Biol*. 2005; 21:659–693. [PubMed: 16212511]
5. O'Connor MB, Umulis D, Othmer HG, Blair SS. Shaping BMP morphogen gradients in the Drosophila embryo and pupal wing. *Development*. 2006; 133:183–193. [PubMed: 16368928]
6. Kishigami S, Mishina Y. BMP signaling and early embryonic patterning. *Cytokine Growth Factor Rev*. 2005; 16:265–278. [PubMed: 15871922]
7. Schmid B, et al. Equivalent genetic roles for *bmp7/snailhouse* and *bmp2b/swirl* in dorsoventral pattern formation. *Development*. 2000; 127:957–967. [PubMed: 10662635]
8. Yelick PC, Abduljabbar TS, Stashenko P. zALK-8, a novel type I serine/threonine kinase receptor, is expressed throughout early zebrafish development. *Dev Dyn*. 1998; 211:352–361. [PubMed: 9566954]
9. Nikaïdo M, Tada M, Takeda H, Kuroiwa A, Ueno N. In vivo analysis using variants of zebrafish BMPR-IA: range of action and involvement of BMP in ectoderm patterning. *Development*. 1999; 126:181–190. [PubMed: 9834197]
10. Nikaïdo M, Tada M, Ueno N. Restricted expression of the receptor serine/threonine kinase BMPR-IB in zebrafish. *Mech Dev*. 1999; 82:219–222. [PubMed: 10354489]
11. Woods IG, et al. The zebrafish gene map defines ancestral vertebrate chromosomes. *Genome Res*. 2005; 15:1307–1314. [PubMed: 16109975]
12. Bauer H, Lele Z, Rauch GJ, Geisler R, Hammerschmidt M. The type I serine/threonine kinase receptor Alk8/Lost-a-fin is required for Bmp2b/7 signal transduction during dorsoventral patterning of the zebrafish embryo. *Development*. 2001; 128:849–858. [PubMed: 11222140]
13. Mintzer KA, et al. Lost-a-fin encodes a type I BMP receptor, Alk8, acting maternally and zygotically in dorsoventral pattern formation. *Development*. 2001; 128:859–869. [PubMed: 11222141]
14. Mullins MC, et al. Genes establishing dorsoventral pattern formation in the zebrafish embryo: the ventral specifying genes. *Development*. 1996; 123:81–93. [PubMed: 9007231]
15. Imai Y, Talbot WS. Morpholino phenocopies of the *bmp2b/swirl* and *bmp7/snailhouse* mutations. *Genesis*. 2001; 30:160–163. [PubMed: 11477698]
16. Sampath TK, et al. Bovine osteogenic protein is composed of dimers of OP-1 and BMP-2A, two members of the transforming growth factor-beta superfamily. *J Biol Chem*. 1990; 265:13198–13205. [PubMed: 2376592]
17. Cui Y, Jean F, Thomas G, Christian JL. BMP-4 is proteolytically activated by furin and/or PC6 during vertebrate embryonic development. *Embo J*. 1998; 17:4735–4743. [PubMed: 9707432]
18. Tucker JA, Mintzer KA, Mullins MC. The BMP signaling gradient patterns dorsoventral tissues in a temporally progressive manner along the anteroposterior axis. *Dev Cell*. 2008; 14:108–119. [PubMed: 18194657]

19. Yeo C, Whitman M. Nodal signals to Smads through Cripto-dependent and Cripto-independent mechanisms. *Mol Cell*. 2001; 7:949–957. [PubMed: 11389842]
20. Gilboa L, Wells RG, Lodish HF, Henis YI. Oligomeric structure of type I and type II transforming growth factor beta receptors: homodimers form in the ER and persist at the plasma membrane. *J Cell Biol*. 1998; 140:767–777. [PubMed: 9472030]
21. Gilboa L, et al. Bone morphogenetic protein receptor complexes on the surface of live cells: a new oligomerization mode for serine/threonine kinase receptors. *Mol Biol Cell*. 2000; 11:1023–1035. [PubMed: 10712517]
22. Graff JM, Thies RS, Song JJ, Celeste AJ, Melton DA. Studies with a *Xenopus* BMP receptor suggest that ventral mesoderm-inducing signals override dorsal signals in vivo. *Cell*. 1994; 79:169–179. [PubMed: 7522972]
23. Koenig BB, et al. Characterization and cloning of a receptor for BMP-2 and BMP-4 from NIH 3T3 cells. *Mol Cell Biol*. 1994; 14:5961–5974. [PubMed: 8065329]
24. Kirsch T, Nickel J, Sebald W. BMP-2 antagonists emerge from alterations in the low-affinity binding epitope for receptor BMPRII. *Embo J*. 2000; 19:3314–3324. [PubMed: 10880444]
25. Macias-Silva M, Hoodless PA, Tang SJ, Buchwald M, Wrana JL. Specific activation of Smad1 signaling pathways by the BMP7 type I receptor, ALK2. *J Biol Chem*. 1998; 273:25628–25636. [PubMed: 9748228]
26. Greenwald J, et al. The BMP7/ActRII extracellular domain complex provides new insights into the cooperative nature of receptor assembly. *Mol Cell*. 2003; 11:605–617. [PubMed: 12667445]
27. Scheufler C, Sebald W, Hulsmeyer M. Crystal structure of human bone morphogenetic protein-2 at 2.7 Å resolution. *J Mol Biol*. 1999; 287:103–115. [PubMed: 10074410]
28. Weber D, et al. A silent H-bond can be mutationally activated for high-affinity interaction of BMP-2 and activin type IIB receptor. *BMC Struct Biol*. 2007; 7:6. [PubMed: 17295905]
29. Aono A, et al. Potent ectopic bone-inducing activity of bone morphogenetic protein-4/7 heterodimer. *Biochem Biophys Res Commun*. 1995; 210:670–677. [PubMed: 7763240]
30. Suzuki A, Kaneko E, Ueno N, Hemmati-Brivanlou A. Regulation of epidermal induction by BMP2 and BMP7 signaling. *Dev Biol*. 1997; 189:112–122. [PubMed: 9281341]
31. Nishimatsu S, Thomsen GH. Ventral mesoderm induction and patterning by bone morphogenetic protein heterodimers in *Xenopus* embryos. *Mech Dev*. 1998; 74:75–88. [PubMed: 9651485]
32. Khokha MK, Yeh J, Grammer TC, Harland RM. Depletion of three BMP antagonists from Spemann's organizer leads to a catastrophic loss of dorsal structures. *Dev Cell*. 2005; 8:401–411. [PubMed: 15737935]
33. Dal-Pra S, Furthauer M, Van-Celst J, Thisse B, Thisse C. Noggin1 and Follistatin-like2 function redundantly to Chordin to antagonize BMP activity. *Dev Biol*. 2006; 298:514–526. [PubMed: 16890217]
34. Piccolo S, Sasai Y, Lu B, De Robertis EM. Dorsoventral patterning in *Xenopus*: inhibition of ventral signals by direct binding of chordin to BMP-4. *Cell*. 1996; 86:589–598. [PubMed: 8752213]
35. Zimmerman LB, De Jesus-Escobar JM, Harland RM. The Spemann organizer signal noggin binds and inactivates bone morphogenetic protein 4. *Cell*. 1996; 86:599–606. [PubMed: 8752214]
36. Piccolo S, et al. The head inducer Cerberus is a multifunctional antagonist of Nodal, BMP and Wnt signals. *Nature*. 1999; 397:707–710. [PubMed: 10067895]
37. Piccolo S, et al. Cleavage of Chordin by Xolloid metalloprotease suggests a role for proteolytic processing in the regulation of Spemann organizer activity. *Cell*. 1997; 91:407–416. [PubMed: 9363949]
38. De Robertis EM. Spemann's organizer and self-regulation in amphibian embryos. *Nat Rev Mol Cell Biol*. 2006; 7:296–302. [PubMed: 16482093]
39. Nguyen VH, et al. Dorsal and intermediate neuronal cell types of the spinal cord are established by a BMP signaling pathway. *Development*. 2000; 127:1209–1220. [PubMed: 10683174]
40. Nguyen VH, et al. Ventral and lateral regions of the zebrafish gastrula, including the neural crest progenitors, are established by a bmp2b/swirl pathway of genes. *Dev Biol*. 1998; 199:93–110. [PubMed: 9676195]

41. Padgett KA, Sorge JA. Creating seamless junctions independent of restriction sites in PCR cloning. *Gene*. 1996; 168:31–35. [PubMed: 8626061]
42. Robu ME, et al. p53 activation by knockdown technologies. *PLoS Genet*. 2007; 3:e78. [PubMed: 17530925]
43. Little SC, Mullins MC. Twisted gastrulation promotes BMP signaling in zebrafish dorsal-ventral axial patterning. *Development*. 2004; 131:5825–5835. [PubMed: 15525664]

Author Manuscript

Author Manuscript

Author Manuscript

Author Manuscript

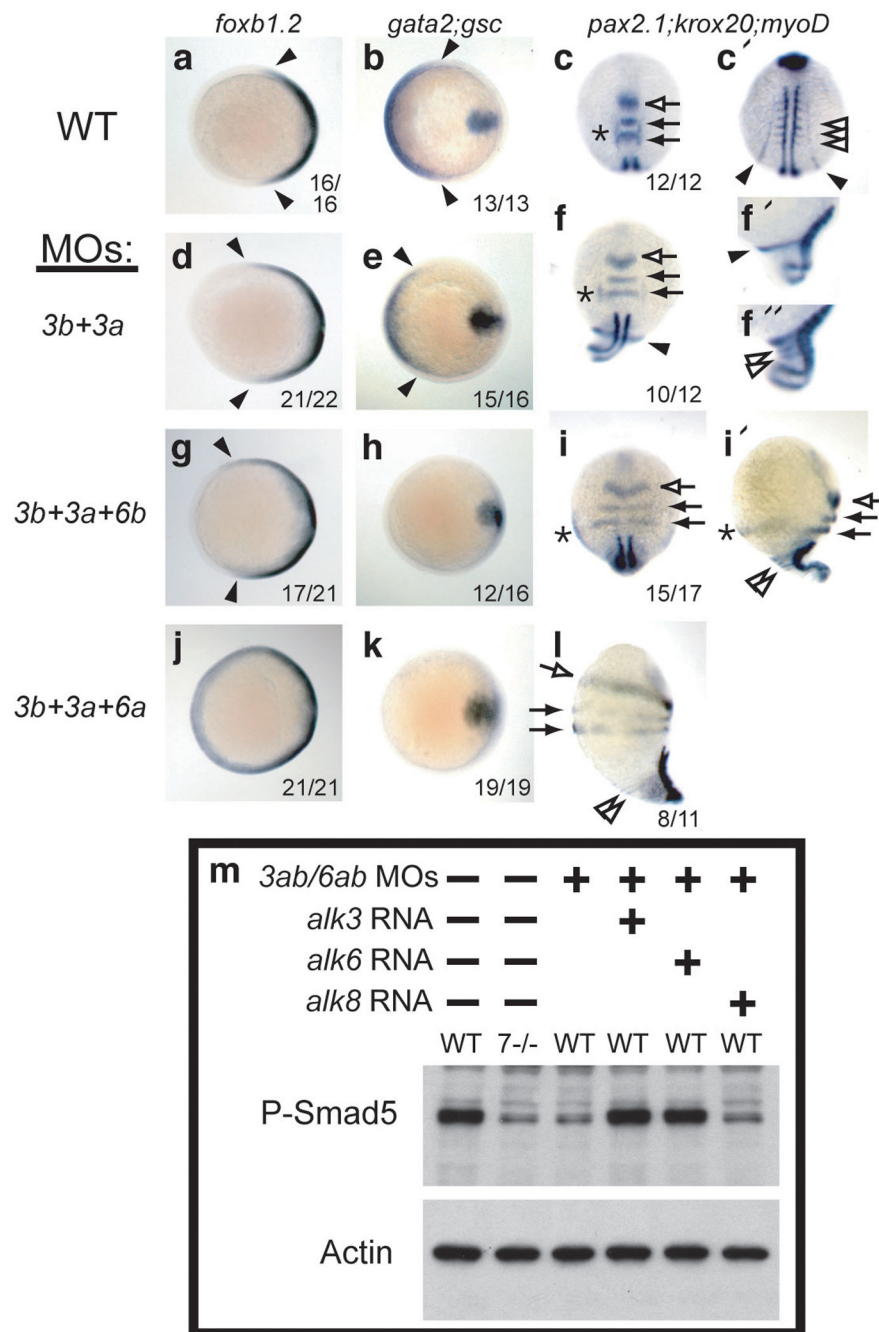


Figure 1. Knockdown of Alk3a/b with Alk6a/b causes increasingly severe dorsalization and loss of P-Smad1/5. **a-l:** Whole mount in situ hybridization of WT embryos (**a-c**) or embryos treated with morpholinos against *alk3b* (4 ng) and *alk3a* (4 ng) together (**d-f**), or combined with *alk6b* MO (2 ng, **g-i**) or *alk6a* MO (6 ng, **j-l**). **a, b, d, e, g, h, j, k:** midgastrulation (75% epiboly), animal pole views, dorsal right, showing dorsal marker *foxb1.2*, (neural ectoderm: **a, d, g, j**), and ventral expression of *gata2* (**b, e, h, k**) with midline mesodermal expression of *gsc* expression as a positive control. **c, f, i, l:** 5 to 6 somite stage (**c, c', f, i, l**, dorsal views

(**c'** more posterior view of embryo pictured in **c**); **f'**, **f'**, **i'**, **l**, lateral views, dorsal to right; anterior up in all images). Intermediate loss of BMP signaling (**f**, **i**) results in expansion of dorsally-derived neural ectoderm (*pax2.1* expression in mid-hindbrain boundary, open arrow, and *krox20* in rhombomeres 3 and 5, closed arrows), and laterally-derived otic placode (*pax2.1*, asterisks) completely extends to the ventralmost domain (**i'**). Elimination of signaling (**l**) causes radial neuralization. Similarly, dorsally-derived paraxial mesoderm (*myoD*, open arrowheads) completely encircles dorsalized embryos (**c**, **f'**, **i'**, **l**), accompanied by reduction of ventrally-derived pronephric mesoderm (*pax2.1*, closed arrowhead, **c'**, **f**, **f'**). **m**: P-Smad5 levels at early gastrulation (shield stage) are reduced by *alk3/6* MO injection (8 ng *alk3b* MO, 4 ng *alk3a* MO, 4 ng *alk6a* MO, 2 ng *alk6b* MO2) to levels observed in completely dorsalized *bmp7* mutants, and rescued by coinjection of *halk3* (10 pg) or *malk6* (2 pg) mRNA, but not by *zalk8* (25 pg). Full blot is shown in Supplementary Information, Figure S6.

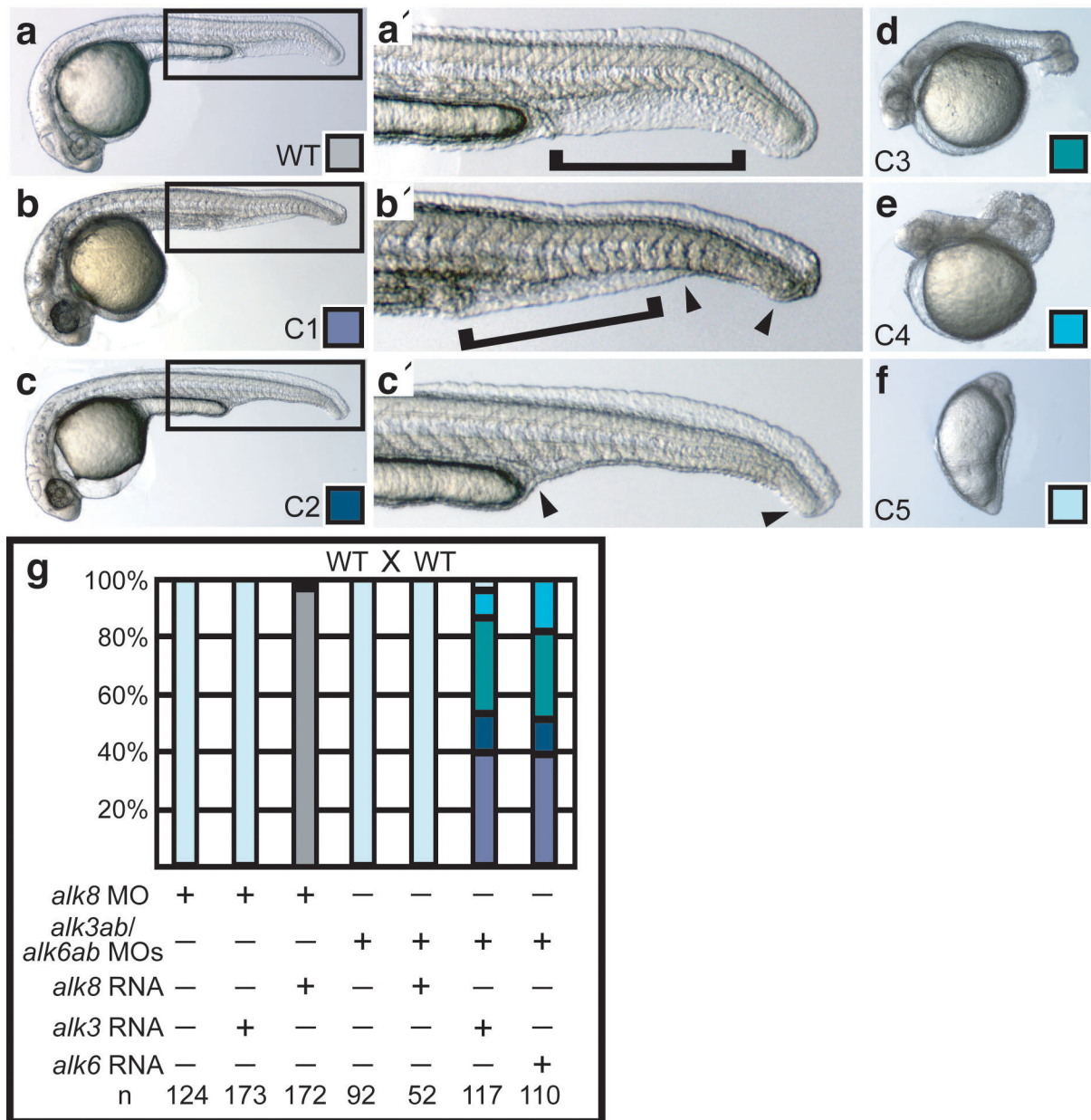


Figure 2. Alk3/6 and Alk8 act nonredundantly and independently. **a–e:** WT (**a**), C1 (**b**), C2 (**c**) (**a'**, **b'**, **c'** magnified views, arrowheads indicate extent of ventral fin tissue loss), C3 (**d**), and C4 (**e**) phenotypes at one day post-fertilization (1 dpf). **f:** severe (C5) dorsalized embryo, shown at the 4-somite stage, does not survive to 1 dpf. **g:** *halk3* mRNA (10 pg) does not rescue *alk8* MO knockdown, whereas *alk8* mRNA does (30 pg); *alk8* mRNA (25 pg) cannot rescue *alk3/6* knockdown (6 ng *alk3b* MO, 4 ng *alk3a* MO, 5 ng *alk6a* MO, 4 ng *alk6b* MO2), whereas *halk3* (10 pg) or *malk6* (2 pg) do.

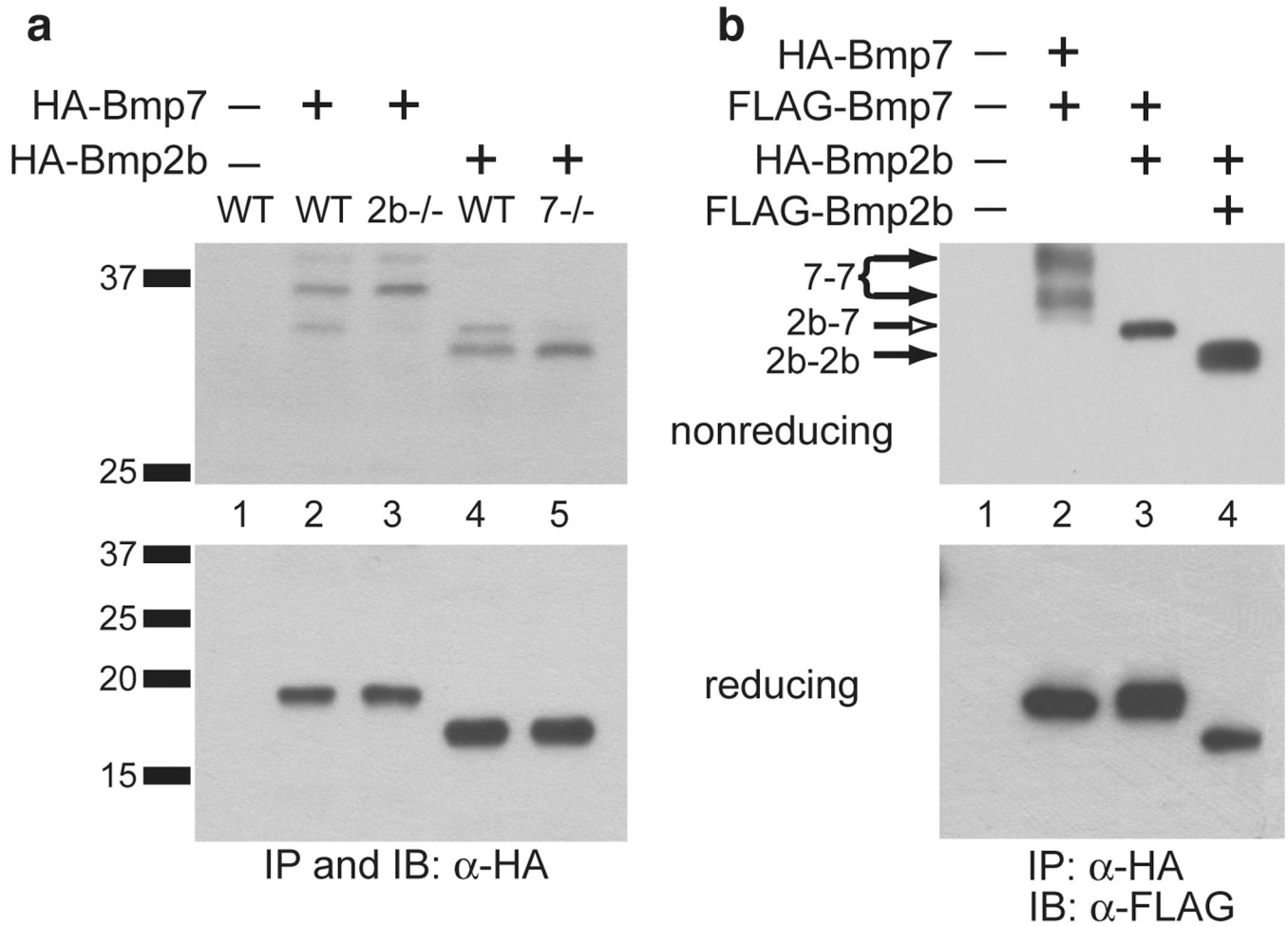


Figure 3. Homo- and heterodimers are present in the zebrafish embryo. **a:** anti-HA immunoblot (IB) of anti-HA IPs from lysates of WT, *bmp2b* MO treated, or *bmp7* protein null mutant embryos expressing HA-tagged Bmp7 or Bmp2b. **b:** anti-HA IP and anti-FLAG IB from embryos co-expressing the indicated ligands. Full blots are shown in Supplementary Information, Figure S6.

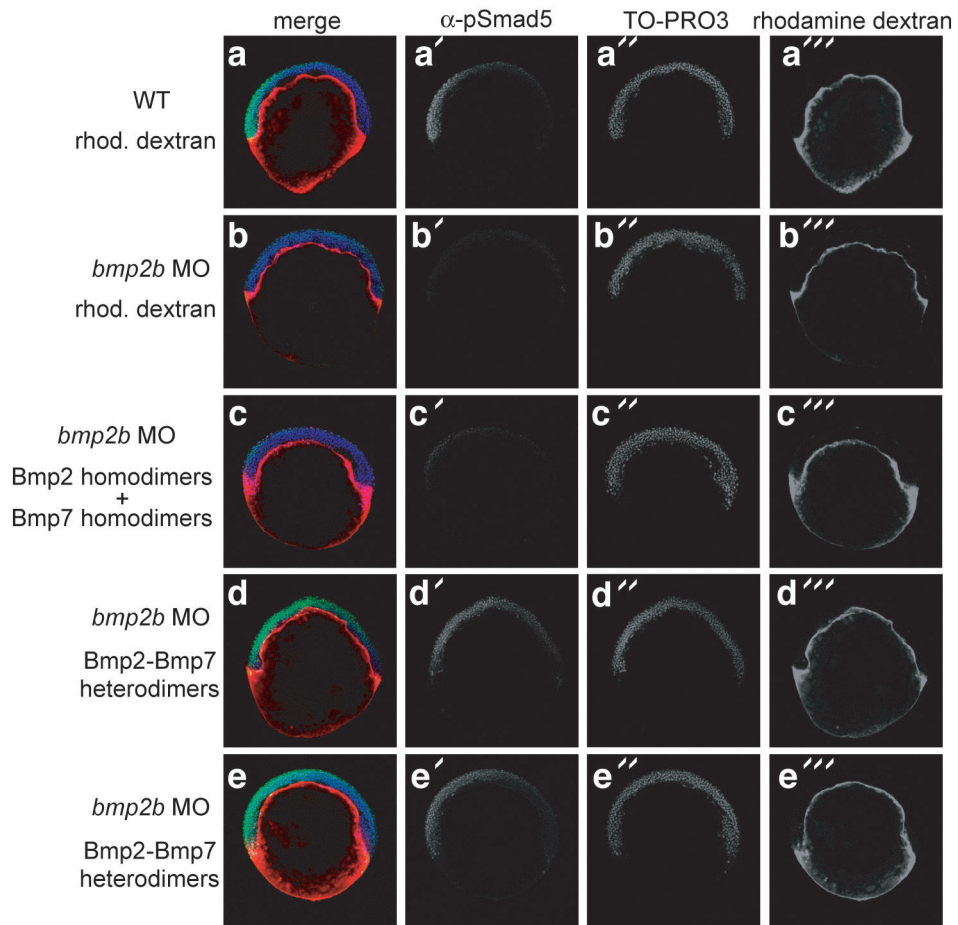


Figure 4. Bmp2-Bmp7 heterodimers pattern the zebrafish embryo. **a:** Yolk cytoplasmic layer of WT embryos was injected with rhodamine dextran between 3 and 4 hpf. P-Smad5 immunostaining reveals nuclear P-Smad5 on the presumptive ventral side. **b–e:** Embryos were injected at the one-cell stage with *bmp2b* MO, then the YCL was injected with rhodamine dextran solution without ligand (**b**, n=10), with an equal concentration of both homodimers (**c**, n=18), or with Bmp2-Bmp7 heterodimers (**d**, **e**, n=15). TO-PRO3 labels nuclei.

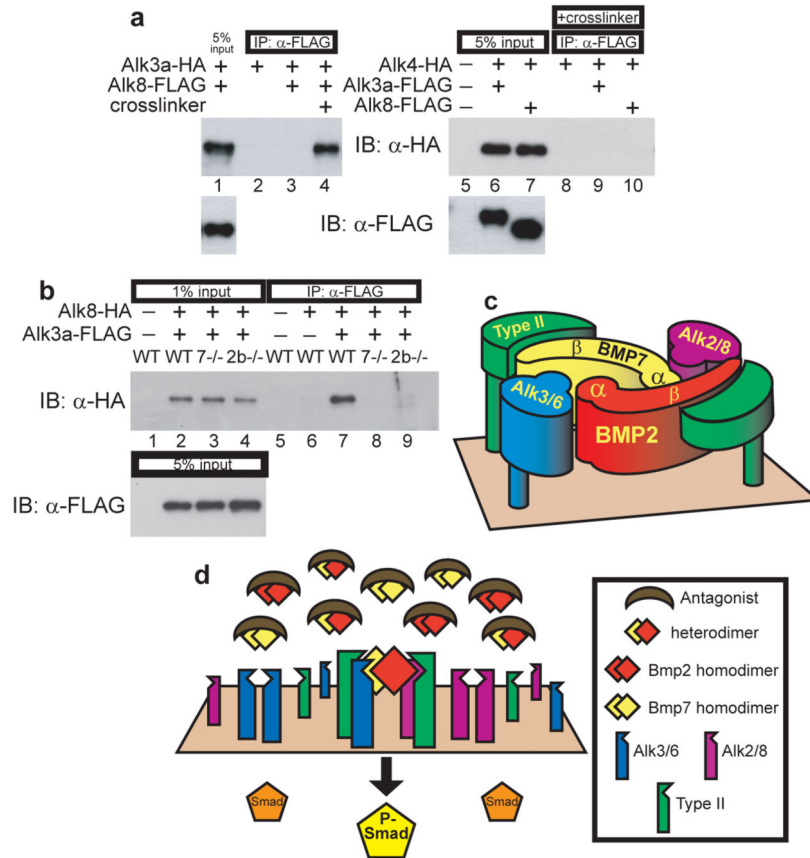


Figure 5.

Alk3a and Alk8 associate in a complex only when Bmp2b and Bmp7 are present. **a:** Anti-FLAG IP and anti-HA IB from lysates of WT embryos expressing Alk3a-HA and Alk8-FLAG treated with or without crosslinker (lanes 1–4), or expressing Alk4-HA with either Alk3a-FLAG or Alk8-FLAG (lanes 5–10). **b:** Anti-FLAG IP and anti-HA IB from lysates of crosslinked WT, *bmp7* protein null mutant, or *bmp2b* MO treated embryos expressing Alk8-HA and Alk3a-FLAG. Full blots are shown in Supplementary Information, Figure S6. **c:** Predicted arrangement of a Bmp2-Bmp7 heterodimer with Alk3/6 and Alk2/8. α : alpha helix, β : beta strands of ligand monomers. **d:** Model of heterodimer-mediated DV patterning.